Utilizing NASIR Galerkin Finite Volume Analyzer for 2D Plane Strain Problems under Static and Vibrating Concentrated Loads

Mohammad T. Alkhamis [1), Saeed-Reza Sabbagh-Yazdi [2), Mahdi Esmaeili [3) and Falah M. Wegian [4)

[1) Assistant Professor, Civil Engineering Department, College of Technological Studies (Kuwait)
[2) Associate Professor, Civil Engineering Department, KNToosi University of Technology, (Iran) SYazdi@kntu.ac.ir
[3) MSc Graduate, Civil Engineering Department, KNToosi University of Technology, (Iran)
[4) Associate Professor, Civil Engineering Department, College of Technological Studies (Kuwait) fmwm@yahoo.com

ABSTRACT

A Numerical Analyzer for Scientific and Industrial Requirements *(NASIR)* software which utilizes novel matrix free Finite Volume is applied for solving plane strain solid state problems on linear triangular element meshes. The developed shape function free Galerkin Finite Volume structural solver explicitly computes stresses and displacements in Cartezian coordinate directions for the two dimensional solid mechanic problems under either static or dynamic loads. The accuracy of the introduced algorithm is assessed by comparison of computed results of cantilever structural elements under static concentrated load with analytical solutions. Then, the performance of the introduced method to solve structural plane strain problem under forced and vibrating loads is demonstrated. The performance of the solver is presented in terms of stress and strain contours as well as convergence behavior of the method.

KEYWORDS: Galerkin finite volume method, Linear triangular element, Stress-strain, Static and vibrating structures.

INTRODUCTION

Over the past decades, a wide variety of numerical methods has been proposed for the numerical solution of partial differential equations. Among them, the Finite Element Method (FEM) has firmly established itself as the standard approach for problems in Computational Solid Mechanics (CSM), especially with regard to deformation problems involving non-linear material analysis (Zienkiewicz and Taylor, 1989).

It is well known that numerical analysis of solids in

incompressible limit could lead to difficulties. For example, fully integrated displacement based lower-order finite elements suffer from volumetric locking, which usually accompanies pressure oscillation in incompressible limit (Bijelonja et al., 2006). Also, there are some difficulties for producing stiffness matrix and shape function in order to increase the convergence rate.

Although certain restrictions on mesh configuration had to be imposed to avoid locking, these restrictions were less severe than those of the equivalent FEM meshes.

The Galerkin Finite Volume Method has similarly established itself within the field of computational fluid dynamics (CFD) (Sabbagh-Yazdi et al., 2008). However,

similar to the FEM, the FVM integrates governing equation(s) over pre-defined control volumes (Zienkiewicz and Taylor, 1989; Sabbagh-Yazdi et al., 2008), which are associated with the elements making up the domain of interest and therefore preserve the conservation properties of the equations. Although, the Finite Volume Method (FVM) was originally developed for fluid flow and heat and mass transfer calculations (Demirdzic and Martinovic, 1999), recently, it is generalized for stress analysis in isotropic linear and non-linear solid bodies. Therefore, the interest for FVM application to the structural analysis problems involving incompressible materials has grown during the recent years. From the results of several benchmark solutions, the FVM appeared to offer a number of advantages over equivalent finite element models. For instant, it can be stated that, unlike the FDM solution, FVM solution is conservative and incompressibility is satisfied exactly for each discretized sub-domain (control volume) of the computational domain (Bijelonja et al., 2006). In principle, because of the local conservation properties, the FVMs should be in a good position to solve such problems effectively. Furthermore, numerical calculation with meshes consisting of triangular cells showed excellent agreement with analytical results. Meshes consisting of quadrilateral FVM cells displayed too stiff behavior, indicating a locking phenomenon (Bijelonja et al., 2006). Therefore, a number of researchers have applied FVMs to problems in CSM over the past decade (Slone et al., 2003) and it is now possible to classify these methods into two approaches, cell-centered and vertex-based ones.

In this paper, a Numerical Analyzer for Scientific and Industrial Requirements (*NASIR)* software which uses the matrix free explicit Galerkin Finite Volume Method on meshes of linear triangular elements (Sabbagh-Yazdi et al., 2008; Sabbagh-Yazdi et al., 2008) is utilized for structural analysis of plane strain problems under static and vibrating loads. The accuracy of the introduced method is assessed by comparison of computed stresses and displacements for two classical cantilever structural elements under static concentrated load with analytical solutions and the performance of the solver is demonstrated in terms of stress and strain contours as well as convergence behavior of the method to the steady state condition. Then, the analysis of a cantilever structural element under forced and free vibrations is performed by the application of the introduced matrix free FVM and the computed results are compared with the analytical solutions.

MATHEMATICAL MODEL

The universal law governing any continuum undergoing motion is given by the general form of Cauchy's equilibrium equations:

$$\rho \ddot{u} = S^T \sigma + b \tag{1}$$

where σ is the stress tensor, b is the body force, ρ is the material density and $\ddot{u}$ is the acceleration.

For two dimensional problems, $\bar{u} = (u_x , u_y)^T$ is the displacement vector and $\sigma = (\sigma_{xx} , \sigma_{yy} , \sigma_{xy})^T$ is the tensor vector. The operator S^T for two-dimensional problems is defined as:

$$S^T = \begin{bmatrix} \dfrac{\partial}{\partial x} & \circ & \dfrac{\partial}{\partial y} \\ \circ & \dfrac{\partial}{\partial y} & \dfrac{\partial}{\partial x} \end{bmatrix}$$

So, the matrix form of Cauchy equations for two-dimensional problems is:

$$\rho\begin{Bmatrix}\dfrac{\partial^2 u_x}{\partial t^2}\\[2mm]\dfrac{\partial^2 u_y}{\partial t^2}\end{Bmatrix}=\begin{bmatrix}\dfrac{\partial}{\partial x}&\circ&\dfrac{\partial}{\partial y}\\[2mm]\circ&\dfrac{\partial}{\partial y}&\dfrac{\partial}{\partial x}\end{bmatrix}\begin{Bmatrix}\sigma_{xx}\\\sigma_{yy}\\\sigma_{xy}\end{Bmatrix}+\begin{Bmatrix}b_x\\b_y\end{Bmatrix}.\qquad(2)$$

For stress-strain relationship, the common Hook equation can be used as:

$$\sigma = D\varepsilon \qquad (3)$$

where D for plane strain problems is the constitutive property matrix and for plane strain problems is:

$$D=\begin{bmatrix}1&\dfrac{\upsilon}{1-\upsilon}&\circ\\[2mm]\dfrac{\upsilon}{1-\upsilon}&1&\circ\\[2mm]\circ&\circ&\dfrac{1-2\upsilon}{2(1-\upsilon)}\end{bmatrix}\times\dfrac{E(1-\upsilon)}{(1+\upsilon)(1-2\upsilon)}.$$

Here, υ is the Poisson ratio and E are the Young modules of elasticity. So, the Cauchy's equilibrium equations in two Cartesian coordinate directions can be written as:

$$\rho\dfrac{\partial^2 u_x}{\partial t^2}=\dfrac{\partial}{\partial x}\left(C_1\dfrac{\partial u_x}{\partial x}+C_2\dfrac{\partial u_y}{\partial y}\right)+\dfrac{\partial}{\partial y}C_3\left(\dfrac{\partial u_x}{\partial y}+\dfrac{\partial u_y}{\partial x}\right)+b_x$$
$$\rho\dfrac{\partial^2 u_y}{\partial t^2}=\dfrac{\partial}{\partial x}C_3\left(\dfrac{\partial u_x}{\partial y}+\dfrac{\partial u_y}{\partial x}\right)+\dfrac{\partial}{\partial y}\left(C_2\dfrac{\partial u_x}{\partial x}+C_1\dfrac{\partial u_y}{\partial y}\right)+b_y \qquad(4)$$

where for plane strain problems:

$$C_1=\dfrac{E(1-\upsilon)}{(1+\upsilon)(1-2\upsilon)},\ \ C_2=\dfrac{E\upsilon}{(1+\upsilon)(1-2\upsilon)},\ \ C_3=\dfrac{E}{2(1+\upsilon)}$$

NUMERICAL FORMULATION

In order to obtain the discrete form of the Cauchy's equation in i direction, the following form is used:

$$\rho\dfrac{\partial^2 u_i}{\partial t^2}=\dfrac{\partial \sigma_{ij}}{\partial x_i}+b_i \qquad (j=1,2)\qquad(5)$$

in which the stresses are defined as:

$$\sigma_{11}=\left(C_1\dfrac{\partial u_x}{\partial x}+C_2\dfrac{\partial u_y}{\partial y}\right)\qquad\sigma_{12}=C_3\left(\dfrac{\partial u_x}{\partial y}+\dfrac{\partial u_y}{\partial x}\right)$$
$$\sigma_{21}=C_3\left(\dfrac{\partial u_x}{\partial y}+\dfrac{\partial u_y}{\partial x}\right)\qquad\sigma_{22}=\left(C_2\dfrac{\partial u_x}{\partial x}+C_1\dfrac{\partial u_y}{\partial y}\right)$$

By the application of the Variational Method, after multiplying the residual of the above equation by the test function ω and integrating over a sub-domain Ω (Figure 1), in the absence of body forces we have:

$$\int_\Omega \omega.\rho\dfrac{\partial^2 u_i}{\partial t^2}d\Omega=\int_\Omega \omega.(\vec\nabla.\vec{F_i})d\Omega \qquad(6)$$

where i direction stress vector is defined as $\vec{F_i}=\sigma_{i1}\hat i+\sigma_{i2}\hat j$.

The terms containing spatial derivatives can be integrated by part over the sub-domain Ω and then equation 6 may be written as:

$$\int_\Omega \omega.\rho\dfrac{\partial^2 u_i}{\partial t^2}d\Omega=[\omega.\vec{F_i}]_\gamma-\int_\Omega(\vec{F_i}.\vec\nabla\omega)d\Omega \qquad(7)$$
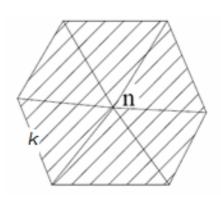
Figure (1): Sub-domain with area Ω_n.

According to the Galerkin method, the weighting function ω can be chosen equal to the interpolation function ϕ. In finite element methods, this function is systematically computed for desired element type and called the shape function. For a triangular type element (with three nodes), the linear shape function, ϕ_k, takes the value of unity at desired node n, and zero at other neighboring nodes k of each triangular element (Figure 2):
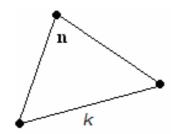
Figure (2): A linear triangular element.

Therefore, the summation of the term $[\,\omega.\vec{F}_i\,]_\gamma$ over the boundary of the sub-domain Ω_n is zero.

The Right Hand Side (RHS) of equation (7) can be discretized as:

$$\int_\Omega (\,\vec{F}_i.\vec\nabla\phi\,)d\Omega \approx -\frac{1}{2}\sum_{k=1}^{N}(\,\tilde{F}_i\vec{\Delta l}\,)_k \qquad (8)$$

Where $\overrightarrow{\Delta l_k}$ is the normal vector of the side k opposite to the node n and $\tilde{F}_i$ is the i direction piece wise constant stress vector at the centre of element associated with the boundary side k (inside the sub-domain Ω_n with N boundary sides).

For a sub-domain formed by linear triangular elements sharing node n, the Left Hand Side (LHS) of equation (7) can be written in discrete form as:

$$\frac{\partial^2}{\partial t^2}\left(\int_\Omega \phi u_i\,d\Omega\right)\approx\frac{\Omega_n}{3}\frac{d^2u_i}{dt^2}\,. \qquad (9)$$

A finite difference approach is applied for discretizaton of the time derivative of i direction displacement, u_i. Hence, the LHS of equation (7) can be written as:

$$\rho\frac{\Omega_n}{3}\frac{d^2u_i}{dt^2}=\rho\left(\frac{u_i^{t+\Delta t}-2u_i^t+u_i^{t-\Delta t}}{(\Delta t)^2}\right)\frac{\Omega_n}{3}\,. \qquad (10)$$

The final discrete form of equation (7) is obtained as:

$$\left(\frac{u_i^{t+\Delta t}-2u_i^t+u_i^{t-\Delta t}}{(\Delta t)^2}\right)=\frac{3}{2\rho\Omega_n}\sum_{k=1}^{N}(\,\tilde{\sigma}_{i1}\Delta y-\tilde{\sigma}_{i2}\Delta x\,)_k \qquad (11)$$

Considering direction $i=1$ as x and $i=2$ as y, the stresses $\tilde{\sigma}_{i1}$ and $\tilde{\sigma}_{i2}$ are computed as:

$$\tilde{\sigma}_{xx}=\left\{C_1\frac{\partial u_x}{\partial x}+C_2\frac{\partial u_y}{\partial y}\right\}\approx\left\{\frac{1}{A_k}\sum_{m=1}^{3}(\,C_1u_x\Delta y-C_2u_y\Delta x\,)_m\right\}$$

$$\tilde{\sigma}_{xy}=\tilde{\sigma}_{yx}=\left\{C_3\left(\frac{\partial u_x}{\partial y}+\frac{\partial u_y}{\partial x}\right)\right\}\approx\left\{\frac{1}{A_k}\sum_{m=1}^{3}(C_3u_x\Delta y-C_3u_y\Delta x)_m\right\} \qquad (12)$$

$$\tilde{\sigma}_{yy}=\left\{C_2\frac{\partial u_x}{\partial x}+C_1\frac{\partial u_y}{\partial y}\right\}\approx\left\{\frac{1}{A_k}\sum_{m=1}^{3}(\,C_2u_x\Delta y-C_1u_y\Delta x\,)_m\right\}$$

where A_k is the area of triangular element (with $m=3$ sides) associated with boundary side k of the sub-domain Ω_n (Figure 3):
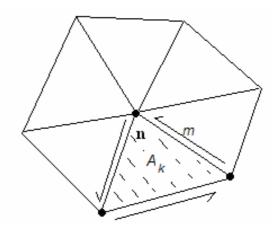

Figure (3): Triangular element with area A_k within the sub-domain Ω_n.

COMPUTATIONAL STEPPING

The time step Δt_n for each control volume can be computed as:

$$\Delta t_n\le\frac{r_n}{c} \qquad (13)$$

where c is the wave velocity. According to the wave velocity, gained by equation (14):

$$c=\sqrt{\frac{E}{\rho(1-\upsilon^2)}}\quad, \qquad (14)$$

here, r_n is the average radius of the equivalent circle that

matches with the desired control volume ($r_n = \Omega_n / P_n$).
For any control volume *n*, this radius can be computed

using area ($r = \Omega_n / \sum_{k=1}^{N_{edge}} (\Delta l)_k$) and perimeter

($P_n = \sum_{k=1}^{N_{edge}} (\Delta l)_k$) of the *2D* control volume.

Due to the variations in sizes of control volume calculations, the allowable time step for computation of dynamic problems for the entire mesh is limited to the minimum associated with the smallest control volume of the domain. However, the large variation in grid size for the triangular mesh will slow down the computations.

In the present work, the local time step of each control volume is used for computation of static problems. In this technique, to accelerate the convergence to steady state conditions, the computation of each control volume can advance using a pseudo time step which is calculated for its own control volume. The use of local time stepping greatly enhances the convergence rate.

LOAD IMPOSING TECHNIQUE

For static problems, an external load is considered as a global source term of Cauchy equations and is added to the LHS of the described FVM formulation. Considering the linear shape function in each triangular cell, the value of the external load at the central node of the control volume is integrated over the control volume and considered at its central node. Fig.4 illustrates the area of the control volume which associates with the imposed load by considering the linear shape function in each triangular cell.

But sudden imposing of the external load would cause some problems for the computational procedure. In order to overcome the problem, gradual load imposing is implemented in the present model using a relaxation coefficient which varies from 0.0 to 1.0 during some computational iterations.
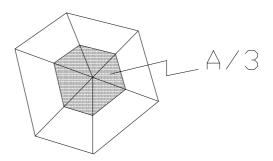

Figure (4): Imposing force area.

$$Relaxation \ \ Coefficient = Min. \left\{ (\frac{I_{step}}{L / \Delta t}), 1. \right\} \quad (15)$$

where I_{step} is the iteration number at the desired stage of the computation, *L* is a length scale that can be assumed as the distance between maximum displacement and the centre of external load or constraint (support location).

For dynamic problems, the still initial condition is considered for the structure. However, for the storage tank case, firstly the hydrostatic condition is satisfied similar to the steady state problems. Then, the time dependent analysis would start.

STATIC LOAD CASE

A standard problem in structural mechanics is that of a fixed-free cantilever supporting an applied load at the free end (Timoshenko, S.P., Goodier, J.N., 1982). The fixed-free cantilever is shown in Fig.4. Here *b=2.0* is the breadth, *L=20.0* the length of the cantilever and *F* the applied load. It is assumed that the depth *d=1.0*. The static solution to this problem is available (Timoshenko and Goodier, 1982) as:

$$d_y = -\frac{4FL^3}{Edb^3} \quad (16)$$

where *E* is Young's modulus and *d* is the height of the cantilever structural element.

Note that the gravity effect is not considered in this

study. The static solution given by the above equation is independent of Poisson's ratio. Therefore, it is applicable to a cantilever undergoing pure flexure, i.e. no axial loads are supported and the out of plane load on the cantilever is zero. Thus for comparison with the analytic solution a zero Poisson's ratio is assumed.

The fixed-free cantilever is considered under a load of *200N* at its free end, as depicted by Fig.5.
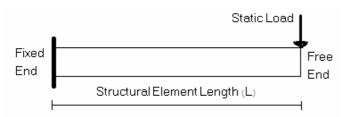

Figure (5): Schematic of flexural deformation test of fixed-free cantilever structural element under static load.

Table (1): Case 1 cantilever structural element specification.

2D Fixed-free specification	value
Load, F	200 N
Length, L	20.0 m
Breadth, b	2.0 m
Density, ρ	2600.0 kg/m^3
Young's modulus, E	10 MPa
Poisson's ratio, υ	0.0

With the parameters as given in Table 1, equation 16 gives the static displacement in *y* direction at the tip of the cantilever as 0.08 m.

In order to provide a better understanding about the effects of gradual load imposing technique, the convergence behavior of the computed displacements is shown in Fig.6 and the root mean square of the computed displacements is shown in Fig.7. As can be seen, the logarithm of root mean square errors of displacements increase by gradual activation of the load in the initial stages of the computation. Then, the logarithms of root mean square errors computed

displacements present a decrease up to 7 orders of magnitude when the load is fully imposed.

The error percentages for the numerical solutions of the problem on various meshes (with various grid spacing sizes) are listed in Table 2. Computed displacements and stress contours are illustrated in Fig.8 and Fig. 9.
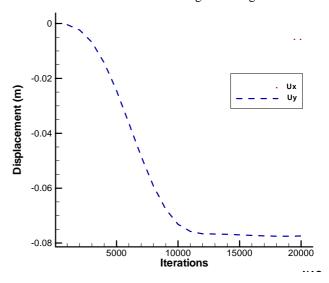

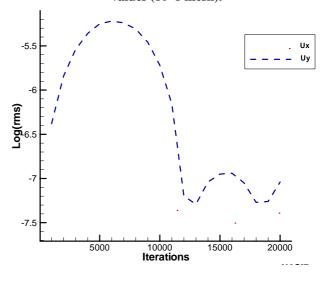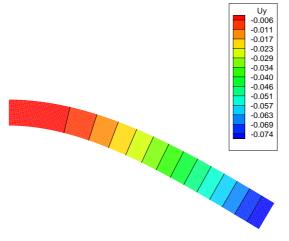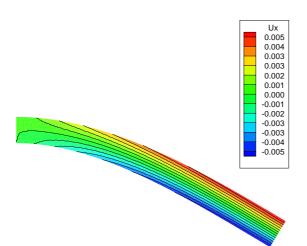**Figure (6): Convergence behavior of tip displacement values (80*8 mesh).**

Figure (7): Convergence behavior of the displacements in terms of the logarithm of root mean square (80*8 meshes).
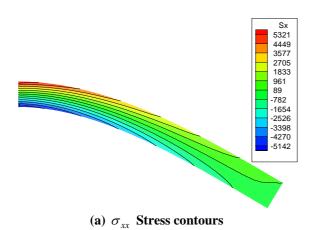
(a) Vertical displacement contours

(b) σ_{yy} Stress contours

(b) Horizontal displacement contours

(c) σ_{xy} Stress contours

Figure (8): Color coded maps of computed displacements.

Figure (9): Color coded maps of computed stresses.

(a) σ_{xx} Stress contours

Table (2): Cantilever structural element error report.

Elements	Vertical displacement at free end	Error for computed values
20*2 triangular	-0.05968	25.4%
40*4 triangular	-0.072169	9.78%
80*8 triangular	-0.077522	3.09%
100*10 triangular	-0.0786	1.7%
200*20 triangular	-0.08007	0.08%

VIBRATING LOAD CASES

In order to present the performance of developed structural solver to model dynamic cases, two test cases which are cantilever structural elements under forced and free vibrations are considered.

a. Forced Vibration

In order to verify the introduced method, a harmonic concentrated load is used at the tip of cantilever structural element with similar specifications to test case2. Fig.10 shows the schematic form of the cantilever structural element loaded by: $F = -200 \sin(0.05t)$.
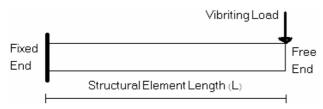

Figure (10): Schematic figure of cantilever structural element harmonic vibrating load.

The analytical solution shows ± 0.08 by the following relation:

$$d_y = -\frac{4FL^3}{Edb^3} \qquad . \tag{17}$$

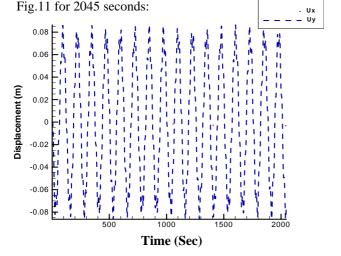The time history of tip displacement is illustrated in Fig.11 for 2045 seconds:

Figure (11): Time history of tip displacement on tip of cantilever structural element under forced vibration.

With a 80*8 triangular mesh, a 2.5% average error is gained. Using finer meshes reduces the error percentages, but the current mesh is efficient enough to be used for dynamic problems.

b. Free Vibration

The cantilever structural element that is used for forced vibration test is utilized for the free vibration test without any damping (Fig.10). The same concentrated load as applied to the forced vibration test is applied and is suddenly released after 40 *sec.* loading. As can be seen in the following figure, the oscillation of the structural element tip continues without any numerical damping and the maximum values of displacement are similar to that obtained under forced vibration test.
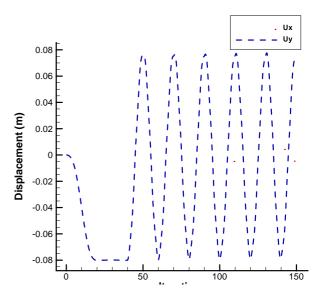

Figure (12): Time history of tip displacement on tip of cantilever structural element under free vibration.

CONCLUSION

In this paper, the Numerical Analyzer for Scientific and Industrial Requirements (*NASIR)* software (Sabbagh-Yazdi et al., 2008; Sabbagh-Yazdi et al., 2008) which utilizes novel explicit matrix free Galerkin Finite Volume Method for the solution of two-dimensional form

of Cauchy equations is applied for structural elements under static and vibrating loads. This computational model solves stress and deformation of plane strain solid mechanics under static and dynamic loads. The performance of the described computational solid mechanic algorithm is examined for various sizes of the meshes for a cantilever structural element under a point load. Since there is no interpolation function in the numerical formulation of the present solver, fine meshes provide more accurate results than coarse meshes.

The present model is examined for some stress-strain structural problems. After verification of the model for static concentrated and uniformly distributed loads on two cantilever structural elements, it is applied for

solution of stresses and deformations of cantilever structural elements under forced and free vibrations. The comparison of the computed results of problems under static and vibrating loads with analytical solution of the test cases presents promising agreement and no unwanted numerical damping is introduced in the computed results of the present explicit structural solver.

The Numerical Analyzer for Scientific and Industrial Requirements (*NASIR)* software which consumes light computational work load because of explicit matrix and shape function free numerical method can easily be extended to three dimensions and applied for solving large deformations of real world solid mechanics problems with complicated geometries.

REFERENCES

Bailey, C., Taylor, G.A., Cross, M. and Chow, P. 1999. Discretisation Procedures for Multi-Physics Phenomena, *Journal of Computational and Applied Mathematics,* 103: 3-17.

Bijelonja, I., Demirdzˇic´, I. and Muzaferija, S. 2006. A Finite Volume Method for Incompressible Linear Elasticity, *Journal of Mechanical Engineering,* 195: 6378-6390.

Demirdzic, I. and Martinovic, D. 1999. Finite Volume Method for Thermo-Elasto-Plastic Stress Analysis, *Computer Methods in Applied Mechanics and Engineering,* 109: 331-349.

Sabbagh-Yazdi, S.R., Alkhamis, M.T., Esmaili, M. and Mastorakis, N.E. 2008. Finite Volume Analysis of Two-Dimensional Strain in a Thick Pipe with Internal Fluid Pressure, *International Journal of Mathematical Models and Methods in Applied Sciences*, 2 (1): 162-167.

Sabbagh-Yazdi, S.R., Mastorakis, N.E. and Esmaili, M. 2008. Explicit 2D Matrix Free Galerkin Finite Volume Solution of Plane Strain Structural Problems on Triangular Meshes, *International Journal of Mathematics and Computers in Simulations*, 2 (4): 1-8.

Sabbagh-Yazdi, S.R., Mastorakis, N.E., Meysami, F. and Namazi- Saleh, F. 2008. 2D Galerkin Finite Volume Solution of Steady Inviscid/Viscous/Turbulent Artificial Compressible Flow on Triangular Meshes, *International Journal of Computers*, 2 (1): 39-46.

Slone, A.K., Bailey, C. and Cross, M. 2003. Dynamic Solid Mechanics Using Finite Volume Methods, Old Royal Naval College, University of Greenwich, *Applied Mathematical Modeling*, 27: 69-87.

Timoshenko, S.P. and Goodier, J.N. 1982. *Theory of Elasticity*, McGraw-Hill, New York.

Zienkiewicz, O.C. and Taylor, R.L. 1989. The Finite Element Method Basic Formulation and Linear Problems, Vol. 1, McGraw-Hill, Maidenhead, UK.